Journal of Neuroscience Methods, 49 (1993) 157–165

NSM 01535

Injection of digitally synthesized synaptic conductance transients to measure the integrative properties of neurons

Hugh P.C. Robinson [a] and Nobufumi Kawai [b]

[a] *Physiological Laboratory, University of Cambridge, Downing St., Cambridge, CB2 3EG (UK) and* [b] *Department of Physiology, Jichi Medical School, Minamikawachi, Tochigi-ken 329-04 (Japan)*

(Received 5 January 1993)
(Revised version received 8 April 1993)
(Accepted 14 April 1993)

Key words: Conductance injection; Synaptic conductance; Current-clamp; Hippocampal neuron

A novel technique was developed for injecting a time-varying conductance into a neuron, to allow quantitative measurement of the processing of synaptic inputs. In current-clamp recording mode, the membrane potential was sampled continuously and used to calculate and update the level of injected current within 60 μs, using a real-time computer, so as to mimic the electrical effect of a given conductance transient. Cellular responses to synthetic conductance transients modelled on the fast (non-*N*-methyl-D-aspartate) phase of the glutamatergic postsynaptic potential were measured in cultured rat hippocampal neurons.

Introduction

The inputs to a neuron consist of focal transients of membrane conductance at the postsynaptic sites, whose magnitude is essentially independent of the postsynaptic response. The output of a neuron is represented by the membrane potential in the cell body or axon. However, the relationship between transient conductance inputs and the resulting trajectory of membrane potential has never been directly measured. The current $I_{syn}(t)$ flowing through the synaptic conductance at a postsynaptic site depends on the postsynaptic membrane potential $V(t)$, according to the equation

$$I_{syn}(t) = g(t)(E_{rev} - V(t)) \quad (1)$$

where $g(t)$ is the time-varying conductance and E_{rev} is the reversal potential for the conductance. In particular, for a given $g(t)$, the current is diminished to zero and then reversed as the membrane is polarized through E_{rev}. $V(t)$ depends upon the complexities of current flow throughout the whole neuron, including $I_{syn}(t)$, active voltage-dependent currents, and currents at other synaptic sites. The interdependence of $I_{syn}(t)$ and $V(t)$ is such that, even for a passive membrane consisting of a linear resistance and capacitance in parallel, the conductance input-voltage output relationship is non-linear. Furthermore, injection of a fixed-current transient, without feedback of the membrane potential cannot, in general, reproduce the effect of a conductance input. Nevertheless, current injection has been the main technique employed to gain experimental insight into the integrative action of mammalian neurons (for a review, see Llinás, 1988). The assumption that synaptic inputs are prescribed current transients also greatly simplifies the problem of calculating voltage responses for

Correspondence: Hugh P.C. Robinson, Physiological Laboratory, University of Cambridge, Downing St., Cambridge, CB2 3EG, UK. Tel.: 0223-333835.

passive membrane, which becomes linear (Rall, 1977). However, as seen from Eqn. 1, this approach can be valid only when the voltage is so far from the equilibrium potential that it can be considered constant. It cannot describe even approximately the action of an inhibitory synapse as the membrane potential ranges on both sides of the reversal potential. The analytical theory of conductance inputs for passive membrane is extremely difficult, and has not so far provided general solutions analogous to those for current inputs (MacGregor, 1968; Barrett and Crill, 1974; Poggio and Torre, 1978; Tuckwell, 1988). Numerical modelling has been the most profitable approach to defining the role of conductance inputs (e.g., Koch et al., 1983; Turner, 1984; Wathey et al., 1992), but relies upon still fragmentary knowledge of the properties and distributions of neuronal membrane conductances.

In order to characterize the integrative action of neurons experimentally, it is necessary to measure the output $V(t)$ in response to exactly specified transients of conductance at defined locations in the cell, which have the same kinetics and reversal potential as natural synaptic conductance transients. Neither voltage-clamp nor current-clamp techniques provide a direct approach to this problem. Voltage-clamp recording, in measuring $g(t)$, necessarily cancels $V(t)$, while current-clamp recording measures $V(t)$ but not $g(t)$. Here, we present a technique for stimulating a neuron, during current-clamp recording, with a current that follows Eqn. 1. This has the effect of simulating a known transient *conductance*, and allows the $g(t)/V(t)$ relationship to be measured explicitly. In this technique, the injected current level is continuously updated according to Eqn. 1 by a real-time computer, using the instantaneous measurement of the membrane potential, a prespecified constant reversal potential and a time template for the conductance derived from voltage-clamp recordings of synaptic currents. The method was applied in small cultured hippocampal neurons to demonstrate the processing of conductance transients mimicking the natural fast excitatory and inhibitory postsynaptic conductances. A preliminary report of this work has appeared elsewhere (Robinson, 1991).

Methods

Dissociated hippocampal neurons were cultured from neonatal rats as described previously (Robinson et al., 1991), and maintained for 1–2 weeks before experiments. Very small (diameter < 12 μm), rounded neurons with few processes were selected for recording. To record natural spontaneous postsynaptic currents, pipettes were filled with the solution: 141 mM CsCl, 5 mM EGTA, 0.5 mM $CaCl_2$, 10 mM HEPES/Na (pH 7.2). The bath solution contained: 150 mM NaCl, 2.8 mM KCl, 0.5 mM $CaCl_2$, 10 mM HEPES/Na (pH 7.2). For conductance injection, the pipette solution consisted of: 141 mM KCl, 0.5 mM $CaCl_2$, 5 mM EGTA, 10 mM HEPES/Na (pH 7.2), and the bath solution of 142 mM NaCl, 2.8 mM KCl, 2 mM $CaCl_2$, 1 mM $MgCl_2$, 10 mM HEPES/Na, 5 mM D-glucose (pH 7.2) to which were added 10 μM CNQX (Tocris Neuramin, Buckhurst Hill, UK), 30 μM APV (Tocris), and 30 μM strychnine (Tokyo Kasei Kogyo Co., Tokyo, Japan). All experiments were at room temperature (23–25°C).

Conductance injection was carried out as follows. Whole-cell recordings (Hamill et al., 1981) were established using a whole-cell patch-clamp amplifier (Axopatch 1-D, Axon Instruments, Foster City, CA) in current-clamp mode. In voltage-clamp mode, the capacitive charging time constant was less than 40 μs. The real-time calculation of the current command signal was performed by a dedicated analog processing board (AS-1, Cambridge Research Systems, Rochester, Kent, UK), which included a 12 MHz 80186 processor, clocks, 512 kbytes memory, and 12-bit analog-to-digital converters (ADC) and digital-to-analog converters (DAC). The settling time constant of the DACs was approximately 1 μs. DAC update and ADC sampling were exactly synchronized using the direct memory access channels of the processor. The membrane potential signal was sampled after passage through an anti-aliasing filter (5 kHz, -3dB Bessel characteristic). Conductance templates were stored in memory at a resolution of 16 bits, and the multiplication, at each time step, by the result of subtracting the voltage from the reversal poten-

tial, was carried out to 28-bit intermediate precision. The 12 most significant bits were written to the DAC connected to the current command input of the amplifier. The arithmetic in each cycle lasted only 4.58 μs, with the remaining time used for handling timers, transferring samples to memory, and update of loop variables. The smallest attainable δt was 58.8 μs, which was used throughout.

Results

Whole-cell voltage-clamp recording from small neurons cultured from rat hippocampus revealed 2 types of spontaneous synaptic current. A glutamatergic excitatory postsynaptic current (e.p.s.c) (Fig. 1a), comprised a fast, non-*N*-methyl-D-aspartate (non-NMDA) receptor-mediated component with a decay time constant (τ) of 1.5–4 ms (Fig. 1a), and a slow, NMDA receptor-mediated phase with a decay τ of 80–150 ms (Eqn. 3) (Fig. 1b), in which single channel openings could clearly be resolved in the whole-cell current (see Robinson et al., 1991). Similar biphasic glutamatergic e.p.s.c.s have been described by Hestrin et al. (1988), Forsythe and Westbrook (1988), Bekkers and Stevens (1989) and Keller et al. (1991), and appear to be a general feature of most mammalian central neurons. An inhibitory postsynaptic current (i.p.s.c.) decayed monoexponentially with a τ of 30–40 ms (Fig. 1c), as described by Segal and Barker (1984).

We found that both the fast phase of the

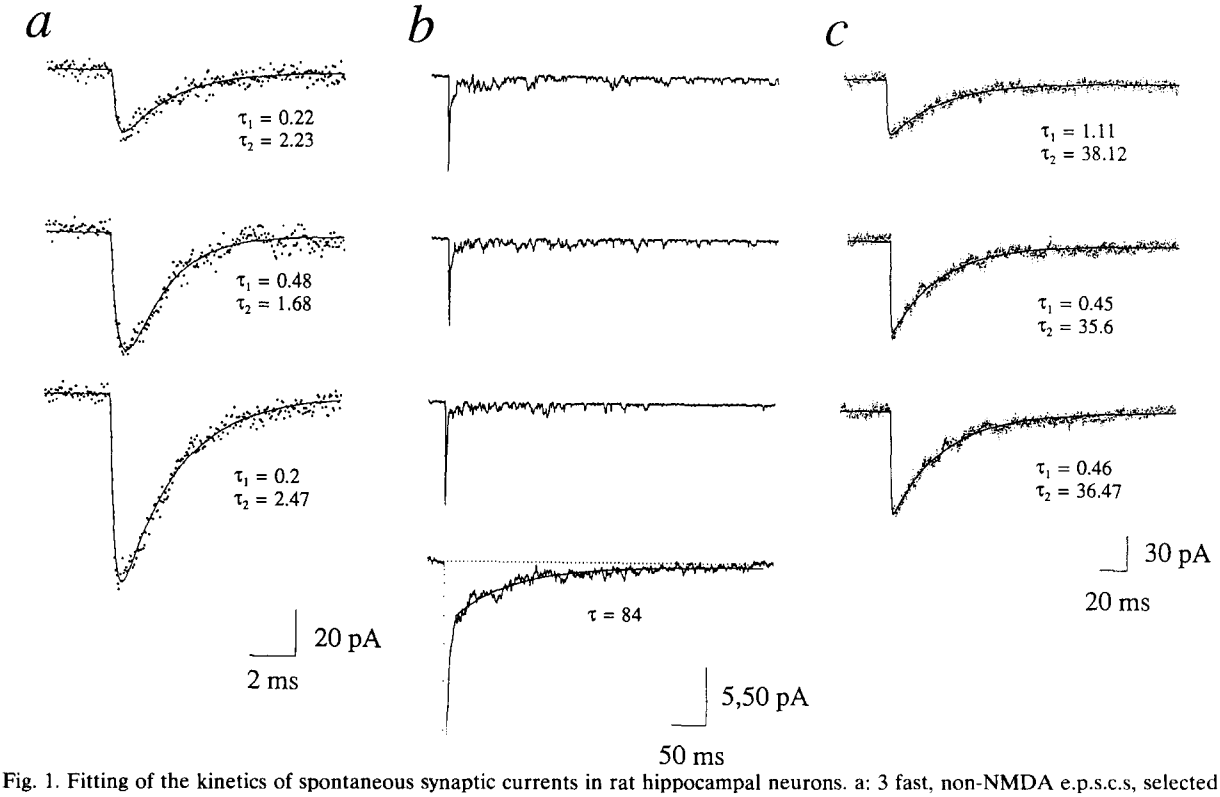

Fig. 1. Fitting of the kinetics of spontaneous synaptic currents in rat hippocampal neurons. a: 3 fast, non-NMDA e.p.s.c.s, selected for the absence of early ensuing NMDA channel openings. Least-squares fits to the equation: $I(t) = K\ (1 - \exp(-t/\tau_1))\ \exp(-t/\tau_2)\ (E_{rev} - V)$ are superimposed with the values of τ_1 and τ_2 indicated. $V = -75$ mV, bandwidth DC -10 kHz (approximate bandwidth of amplifier and recording system, resampled at 25 kHz). b (3 top traces): spontaneous e.p.s.c.s, with the characteristic biphasic appearance of the non-NMDA (fast)/NMDA (slow, noisy) glutamatergic e.p.s.c. Single channel openings may be seen in the NMDA phase. (lower trace): ensemble average of 30 aligned spontaneous e.p.s.c.s, with a single exponential fit of $\tau = 84$ ms to the slow (NMDA) phase. $V = -75$ mV, bandwidth DC -2 kHz (Gaussian). c: 3 i.p.s.c.s, with fits as in (a). $V = -70$ mV, bandwidth DC -10 kHz, as in (a).

e.p.s.c and i.p.s.c were well fitted by a product of 2 exponential functions, so that the underlying conductance transients, $g(t)$, could be written as

$$g(t) = K \cdot \left(1 - \exp\frac{-t}{\tau_1}\right) \cdot \exp\frac{-t}{\tau_2}. \qquad (2)$$

Assuming that $g(t)$ is independent of V, the current $I(t)$ flowing at the synaptic site should be given by substituting Eqn. 2 for $g(t)$ in Eqn. 1. This assumption is reasonable for the fast glutamate e.p.s.c., which shows only a 10% change in decay τ over the range -100 mV to 0 mV (Keller et al., 1991). To inject conductance transients, we used the discrete time approximation to Eqn. 1: $I_{t+\delta t} = g_t \ (E_{rev} - V_t)$, to determine the commanded current in current-clamp recording mode. At time $t + \delta t$, the commanded current level was updated to the product of the conductance value in the template for time t and the result of subtraction of the potential measured at time t from the reversal potential E_{rev}. This feedback loop has the effect of creating a current source which well approximates the effect of the synaptic conductance $g(t)$ when δt is small. In the present experiments, δt was fixed at 58.8 μs. To confirm the accuracy of the conductance synthesis, we injected conductance transients of the form specified by Eqn. 2 with $\tau_1 = 2$ ms and $\tau_2 = 15$ ms, into a model passive cell. The resulting voltage response was very close to the expected response, calculated by integrating the differential equation for the circuit numerically (Fig. 2).

Fig. 3a shows the injection of a conductance transient modelled on that of the fast e.p.s.c, with a reversal potential of 0 mV. For all conductance injection experiments, the pipette contained a predominantly potassium chloride solution (see Materials and methods), while CNQX, APV, strychnine and magnesium were added to the bath. The intention was to block natural synaptic events without impairing the function of voltage-dependent channels which react to synaptic conductance inputs under physiological conditions; it should be noted that strychnine is an effective blocker not only of glycine receptors, but also of $GABA_A$ receptors at the concentration used (30 μM) (Shirasaki et al., 1991). The measured potential is shown superimposed on the expected

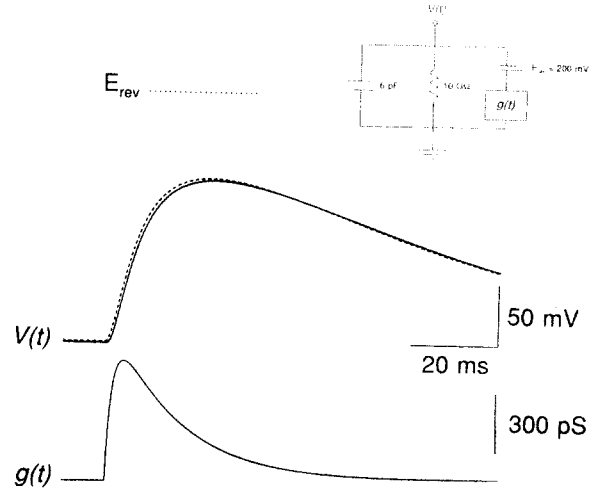

Fig. 2. Conductance injection in a model cell. $g(t)$ was specified by Eqn. 2, with $K = 900$ pS, $\tau_1 = 2$ ms, $\tau_2 = 15$ ms, $E_{rev} = 200$ mV (indicated by a dotted line). The parameters of the model cell are shown in the inset. The solid $V(t)$ trace shows the measured response (average of 10 trials), while the dashed trace shows the expected response calculated by numerical integration (Euler integration, time step 1 μs).

passive response calculated by numerical integration, using the values for cell input resistance and capacitance determined by small hyperpolarizing current steps from rest (see Fig. 3a inset). This reveals a non-linear active response due to voltage-dependent inward current. The injected current is the product of the time-varying potential driving force and the conductance template, and reaches its peak approximately 0.5 ms before the peak of conductance, then falls biphasically before rising again in a small, late peak. Thus, current of a similar time course should flow through the non-NMDA channels during a synaptic potential in the unclamped active membrane. In Fig. 3b, a conductance template based on the slower kinetics of an inhibitory postsynaptic event, and a reversal potential of -60 mV, was injected repeatedly as the membrane potential was changed between -100 and -25 mV by background current injection, illustrating the reversal of the artificially induced transients.

The relationship between the amplitude of a fast glutamate-like conductance transient and the depolarization was investigated by varying K (Fig. 4a). At potentials near to rest, the form of re-

sponses is as expected for a passive membrane, and the peak of each response showed the gradual sublinearity expected as the driving force was reduced by approaching E_{rev}. Around -35 mV, a graded action potential appeared, whose peak becomes higher and earlier with increasing K. Graded action potentials are also observed in small cultured hippocampal neurons when stimulated by conventional current injection (Johannson et al., 1992). From the plot of the peak of $V(t)$ against K (Fig. 4b), the resistance of this cell appears to be higher in the depolarizing direction than measured at rest, possibly due to the presence of inward rectifier K^+ channels. Similar peak $V(t) - K$ relationships were found in 3 other neurons. Fig. 5 shows the effect of varying the kinetics of the conductance transient, in the same neuron as in Fig. 4. When the 2 time constants in Eqn. 2 were multiplied by the same scaling factor, (scaling in time only, without change in the peak conductance), the maximum depolarization at each value of K increased markedly as the kinetics were scaled from $\tau_1 = 0.5$, $\tau_2 = 2$ ms, up to $\tau_1 = 3$, $\tau_2 = 12$ ms, but showed comparitively little further change at $\tau_1 = 4$, $\tau_2 = 16$ ms.

Temporal summation was investigated in 1 neuron by varying the separation between 2 identical excitatory conductance transients (Fig. 6). For $K = 300$ pS, separations of 10 ms and over were subthreshold for eliciting an action potential. At smaller separations, however, a late action potential was elicited, which increased in amplitude to a maximum at 5 ms separation, declining sharply again as the separation was decreased further, though the peak value of injected conductance continued to increase. Thus, there was a sharply defined optimal separation of 5 ms. The temporal summation experiments

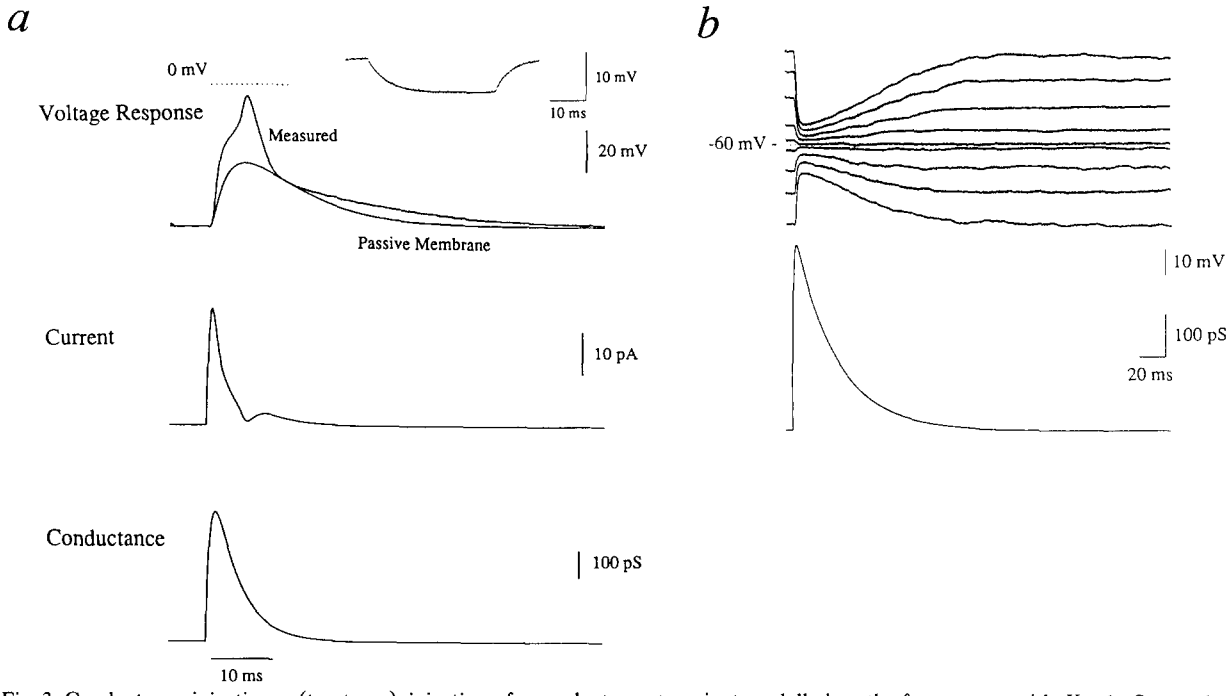

Fig. 3. Conductance injection. a (top trace): injection of a conductance transient modelled on the fast e.p.s.c., with $K = 1$ nS, $\tau_1 = 1$, $\tau_2 = 4$, $E_{rev} = 0$ mV; (top trace): measured voltage response superimposed on the expected response (calculated by numerical integration) if the cell comprised a 3.79 GΩ resistor and a 2.2 pF capacitor in parallel; values measured using 1.4 pA hyperpolarizing current steps from rest (inset). (middle trace): the (commanded) current injected during the transient, determined by the equation: $I_{t+\delta t} = g_t (E_{rev} - V_t)$. δt was 58.8 μs. b: voltage responses to injection of a g_t template modelled on the i.p.s.c. (bottom trace): $K = 500$ pS, $\tau_1 = 1$ ms, $\tau_2 = 30$ ms, $E_{rev} = -60$ mV. The resting membrane potential was varied for each different voltage response by injection of an additional constant background current. Cell resistance, 3.5 GΩ; capacitance, 1.71 pF.

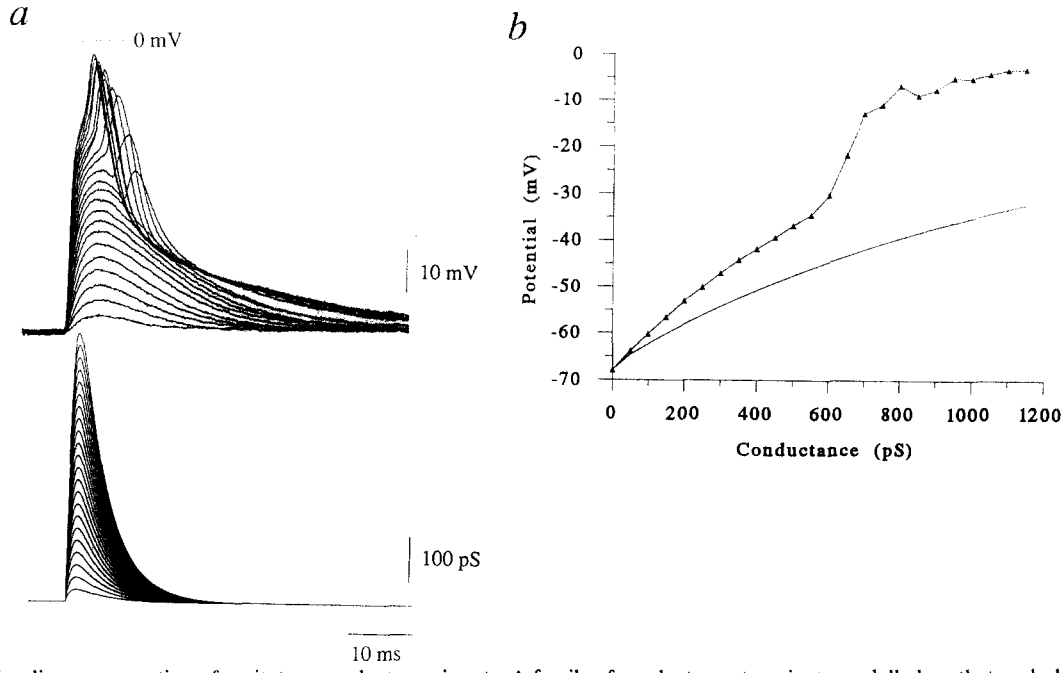

Fig. 4. Non-linear summation of excitatory conductance inputs. A family of conductance transients modelled on that underlying the fast glutamatergic e.p.s.c. ($\tau_1 = 1$ ms, $\tau_2 = 4$ ms, $E_{rev} = 0$ mV) was injected into a neuron with a resting potential of -65 mV. Each injection was separated by 10 s for recovery, and K was stepped from 50 pS to 1.1 nS in steps of 50 pS. a: measured potential responses (top) and conductance transients (bottom). b: peak membrane potential during each transient as a function of the K scaling value. Triangles: measured values. Solid line: computed responses for passive cell ($R = 3.79$ GΩ, C = 2.2 pF).

showed a much higher variation in spike amplitude when compared to injection of a single conductance transient eliciting the same maximum response (not shown), and the greatest variation was at the optimal separation.

Discussion

The accuracy of the present method depends upon sufficiently fast current injection by the current-clamp amplifier, such that the commanded current is not filtered significantly, and on the delay with which the current command is updated by the real-time computer, δt, which should be short enough not to give rise to aliasing of the voltage transient. The close agreement of the time course and amplitude of voltage transients with the calculated transients in the model cell (Fig. 2), implies that neither source of error was significant for passive responses to the synthetic synaptic conductance transients. In the neurons examined, the 17 kHz sampling rate used was sufficient not to alias measured active responses, and current-clamp showed a fast time constant of about 50 μs. However, for cells with much larger active currents, for example at a later stage of development, it would be important to use a conventional amplifier designed for high-speed current-clamp with a voltage follower at the input stage, instead of a patch-clamp amplifier, and also to decrease δt further to prevent aliasing of the sampled potential.

We used the product of 2 exponentials (Eqn. 2) to describe the form of synaptic conductance changes, and showed that such a function provides good fits to natural synaptic inhibitory and fast excitatory currents in these cells. When the ratio $\tau_1 : \tau_2$ is large, this function becomes close to the difference (or convolution) of 2 exponentials, which may be expected theoretically if transmitter release is effectively pulsatile and synaptic channels have a single open and a single closed state. However, the method permits any

form of conductance transient template to be used; indeed, natural synaptic currents recorded at a constant potential V and scaled down by a factor of $(E_{rev} - V)$, could be used directly as the conductance template.

The time course of the current injected during conductance injection can differ radically from that of the conductance transient, as seen in Fig. 3, owing to the dynamic sensitivity of the current to the potential. As expected, conductance injection gave the same saturating and reversible responses as do natural synaptic conductances (Figs. 3 and 4). It thus offers a considerably more realistic way to measure neuronal stimulus–response characteristics than does prescribed current injection. The relationship of K (peak conductance) to $V(t)$ showed significant non-linearity (Fig. 4), in the passive range of membrane potential as well as in the range of active responses.

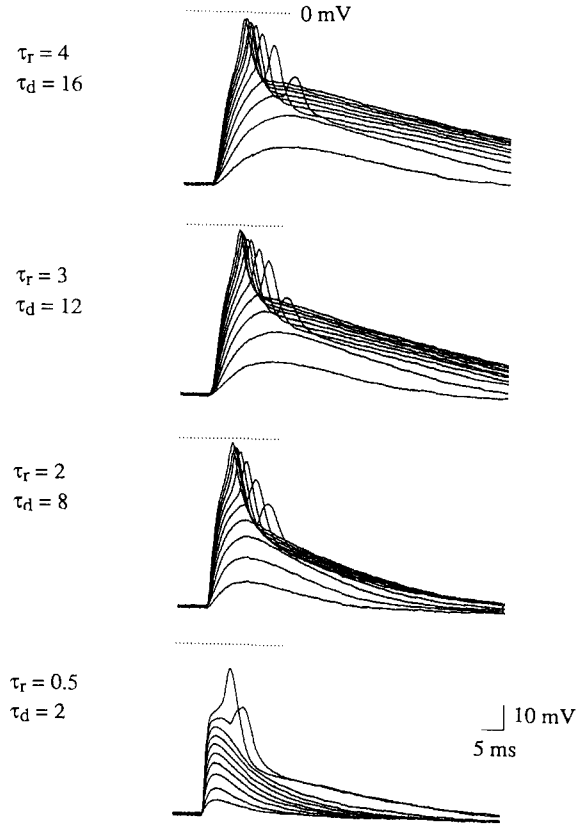

Fig. 5. Effect of variation of kinetics of transient conductance inputs. Families of conductance transients were injected as in Fig. 3. For each set of values of τ_1 and τ_2 (indicated on the left), K was stepped from 100 pS to 1 nS in increments of 100 pS.

Temporal summation of 2 excitatory conductance transients revealed an even greater non-linearity of response (Fig. 6), with a sharply defined optimum interval between transients for eliciting the maximum depolarization, in this case at about 5 ms. This phenomenon could lead to a resonant amplification of conductance inputs at a preferred frequency. The variability of the response even at the optimum interval could be explained if the second conductance transient occurs when the membrane has been brought close to a relatively non-linear state by the first transient. The second response would therefore become a sensitive function of the membrane potential reached, and would be highly susceptible to perturbation by membrane current noise.

We have demonstrated that conductance injection allows the functional role of synaptic conductances characterized by voltage-clamp to be studied directly and quantitatively in unclamped excitable cells, obviating a full reconstruction of the membrane currents by numerical modelling. The site of conductance injection is the site of the electrode, and simulation of remote dendritic synaptic conductance transients would require appropriate placement of the electrode. Specific chemical effects of ions such as Ca^{2+} flowing during natural conductance transients are not, of course, duplicated by the present method; this could, however, be useful in differentiating between chemically dependent and purely electrical components of synaptic responses. The technique could be extended in a number of ways. Using the much greater processing speeds of the presently available digital signal processor chips, it would be possible to measure the interaction of several time-dependent conductances with different reversal potentials, as in simultaneous excitatory and inhibitory synaptic input. One additional multiplication per δt with a value in a look-up table would enable simulation of permeabilities with non-linear instantaneous current-voltage relationships, such as the NMDA receptor channel (Mayer et al., 1984; Nowak et al., 1984). The injection of conductances with voltage-dependent

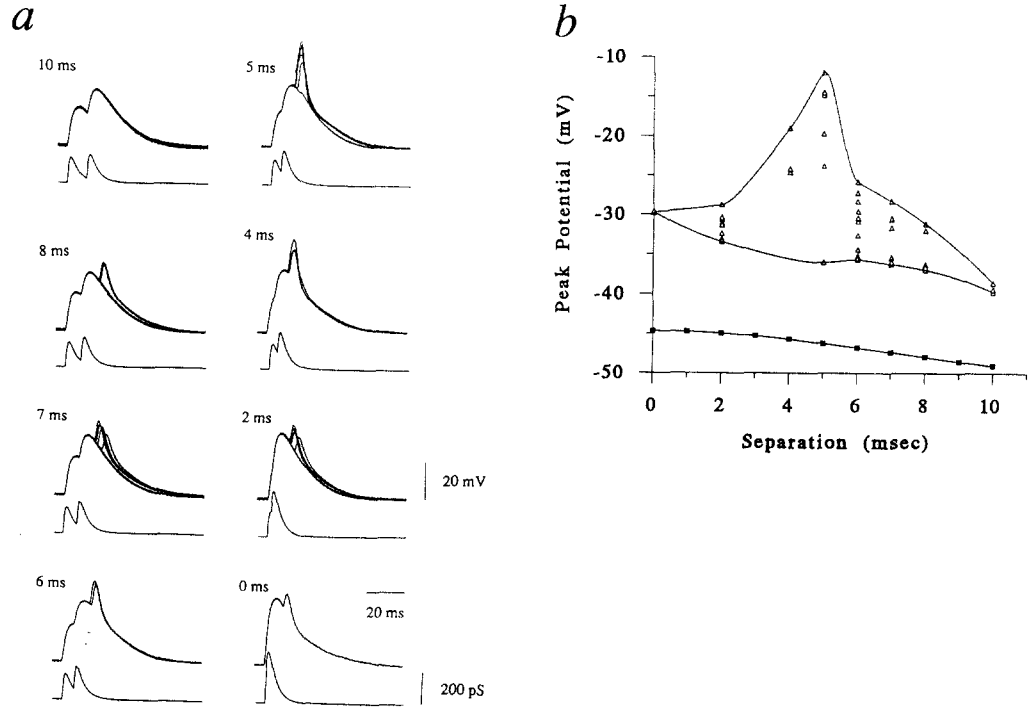

Fig. 6. Temporal summation of excitatory conductance inputs. a: the sum of 2 identical conductance transients ($K = 300$ pS, $\tau_1 = 1$ ms, $\tau_2 = 4$ ms, $E_{rev} = 0$ mV) offset by various intervals between 0 and 10 ms was injected into a neuron. Three to 10 records were acquired at each interval, with 10 s between trials. b: the peak membrane potential reached was plotted as a function of the separation between the summed conductance transients (open triangles). Solid lines indicate the envelope of the response, which showed a marked optimum at 5 ms separation between conductance transients. Filled squares: computed response of the passive circuit of the neuron.

kinetics described by the conventional model (Hodgkin and Huxley, 1952) would be feasible if the rate equations could be integrated accurately in real time. Injection of negative conductance could be used to cancel or titrate intrinsic conductances.

Acknowledgements

We thank Prof. Vincent Torre, Universitá di Genova, for his comments. This work was supported by a grant from the Japanese Ministry of Science and Culture, No. 63060006.

References

Barrett, J.N. and Crill, W.E. (1974) Influence of dendritic location and membrane properties on the effectiveness of synapses on cat motoneurones. J. Physiol., 239: 325–345.

Bekkers, J.M. and Stevens, C.F. (1989) NMDA and non-NMDA receptors are colocalized at individual excitatory synapses in cultured rat hippocampus. Nature, 341: 230–233.

Forsythe, I.D. and Westbrook, G.L. (1988) Slow excitatory postsynaptic currents mediated by *N*-methyl-D-aspartate receptors on cultured mouse central neurones. J. Physiol. (Lond.), 396: 515–533.

Hamill, O.P., Marty, A., Neher, E., Sakmann, B. and Sigworth, F.J. (1981) Improved patch-clamp techniques for high-resolution current recording from cells and cell-free membrane patches. Pflügers Arch., 391: 85–100.

Hestrin, S., Nicoll, R.A., Perkel, D.J. and Sah, P. (1990) Analysis of excitatory synaptic action in pyramidal cells using whole-cell recording from rat hippocampal slices. J. Physiol. (Lond.), 422: 203–225

Hodgkin, A.L. and Huxley, A.F. (1952) A quantitative description of membrane current and its application to conduction and excitation in nerve. J. Physiol. (Lond.), 117: 500–544.

Johansson, S., Friedman, W. and Århem, P. (1992) Impulses and resting membrane properties of small cultured rat hippocampal neurons, J. Physiol. (Lond.), 445: 129–140.

Llinás, R.R. (1988) The intrinsic electrophysiological properties of mammalian neurons: insights into central nervous system function. Science, 242: 1654–1664.

Keller, B.U., Konnerth, A. and Yaari, Y. (1991) Patch clamp analysis of excitatory synaptic currents in granule cells of rat hippocampus. J. Physiol. (Lond.), 435: 275–293.

Koch, C., Poggio, T. and Torre, V. (1983) Nonlinear interactions in a dendritic tree: localization, timing, and role in information processing. Proc. Natl. Acad. Sci. (USA), 80: 2799–2802.

MacGregor, R.J. (1968) A model for responses to activation by axodendritic synapses. Biophys. J., 8: 305–318.

Mayer, M.L., Westbrook, G.L. and Guthrie, P.B. (1984) Voltage-dependent block by Mg^{2+} of NMDA responses in spinal cord neurones. Nature, 309: 261–263.

Nowak, L., Bregestovski, P., Ascher, P., Herbet, A. and Prochiantz, A. (1984) Magnesium gates glutamate-activated channels in mouse central neurons. Nature, 307: 462–465.

Poggio, T. and Torre, V. (1978) A new approach to synaptic interactions. In: R. Heim and G. Palm (Eds.), Approaches to complex systems, Springer, Berlin, pp. 89–115.

Rall, W. (1977) Core conductor theory and cable properties of neurons. In: E.R. Kandel (Ed.), Handbook of Physiology, The Nervous System, Vol. 1, Section 1, Am. Physiol. Soc., Bethesda, MD.

Robinson, H.P.C. (1991) Kinetics of synaptic conductances in mammalian central neurons. Neurosci. Res., Suppl. 16: VI.

Robinson, H.P.C., Sahara, Y. and Kawai, N. (1991) Nonstationary fluctuation analysis and direct resolution of single channel currents at postsynaptic sites. Biophys. J., 59: 295–304.

Segal, M. and Barker, J.L. (1984) Rat hippocampal neurons in culture: voltage-clamp analysis of inhibitory synaptic connections. J. Neurophysiol., 52: 469–487.

Shirasaki, T., Klee, M.R., Nakaye, T. and Akaike, N. (1991) Differential blockade of bicuculline and strychnine on GABA- and glycine-induced responses in dissociated rat hippocampal pyramidal cells. Brain Res., 561: 77–83.

Tuckwell, H.C. (1988) Introduction to Theoretical Neurobiology, Vol. 2, Nonlinear and Stochastic Theories, Cambridge University Press, Cambridge, UK, 265 pp.

Turner, D.A. (1984) Conductance transients onto dendritic spines in a segmental cable model of hippocampal neurons. Biophys. J., 46: 85–96.

Wathey, J.C., Lytton, W.W., Jester, J.M. and Sejnowski, T.J. (1992) Computer simulations of EPSP-spike (E-S) potentiation in hippocampal CA1 pyramidal cells. J. Neurosci., 12: 607–618.